Eur. Phys. J. Special Topics **225**, 1245–1254 (2016)

DOI: 10.1140/epjst/e2016-02669-8

THE EUROPEAN PHYSICAL JOURNAL SPECIAL TOPICS

Regular Article

Dynamics of the fraction of drug particles near the release boundary

Justifying a stretched exponential kinetics in Fickian drug release

E.V. Christidi[1] and G. Kalosakas[1,2]

[1] University of Patras, Materials Science Dept., Rio 26504, Greece
[2] Crete Center for Quantum Complexity and Nanotechnology (CCQCN), Physics Dept., University of Crete, 71003 Heraklion, Greece

Received 28 March 2016 / Received in final form 26 July 2016
Published online 30 September 2016

Abstract. We consider a drug release formulation and investigate the evolution of the fraction of drug molecules that are sufficiently close to the release boundary, in order to check the validity of the assumption underlying the theoretical derivation of a stretched exponential (Weibull) release kinetics. Diffusion-controlled drug release from spheres and slabs is considered. Both analytical results and Monte Carlo simulations are used to calculate the evolution of diffusive drug particles. We find that the fraction of drug molecules near to an exit, as a function of time, follows an inverse power-law in a substantial part of the release problem (from around 1–5% up to at least 80% of the release), justifying an approximate description of the release kinetics through a stretched exponential function.

1 Introduction

Drug release kinetics is conveniently provided through the stretched exponential (Weibull) function. In various experiments it has been found that the Weibull function successfully describes the observed release profiles. Examples include the release of diltiazem hydrochloride and diclofenac sodium, used as model drugs, in various formulations, as well as a number of more than twenty cases of published release data for a variety of drugs [1], vancomycin release from calcium phosphate ceramics [2], epidermal growth factor release from smart multilayer devices [3], and in-vitro release of the model anticancer drug 5-fluorouracil from microporous zeolites [4]. In a comparative study, kinetic analysis of the release of a few dozens of drugs from more than one hundred nanoparticle formulations revealed that the Weibull model was one of the most suitable general model for describing experimental release profiles [5]. Furthermore, the stretched exponential function has been widely used to describe numerically obtained release curves [6–16]. In this case the fractional release can be approximately fitted through [17]:

$$\frac{M_t}{M_\infty} = 1 - e^{-(t/\tau)^b} \tag{1}$$

where M_t is the amount of drug released at time t, M_∞ is the total amount of drug released at infinite time, and b, τ are the two stretched exponential parameters. This equation, Eq. (1), has the advantage over other popular descriptions, like the Higuchi [18,19] or Peppas [20–23] models, that it exhibits the proper asymptotic behavior of the release at relatively long times. Such a qualitatively appropriate description of the whole release profile is achieved without introducing more parameters than for example the well known and extensively used power-law model. As a result the Weibull model is widely used in dissolution and release studies [1–17,24–28].

Kosmidis et al. have provided in [6] a physical reasoning for the justification of a stretched exponential release. The presented argument goes as follows [6]: Consider that initially the drug delivery device is uniformly loaded (homogeneous drug concentration). During the release progress, drug particles close to the release boundary are removed from the formulation and a concentration gradient is formed. Thus the fraction of drug molecules near the boundary is decreasing with time. If N is the number of drug particles within the formulation at time t, then the escape rate is

$$\frac{dN}{dt} = -\alpha f_b N \tag{2}$$

where $f_b(t)$ is the fraction of drug particles that can exit through the boundary per unit of time and α is a proportionality constant. The $f_b(t)$ is a decreasing function of time, but its exact form is unknown. A stretched exponential release kinetics, Eq. (1), is obtained if one *assumes* that the function $f_b(t)$ behaves as an inverse power law

$$f_b(t) \sim t^{-m}. \tag{3}$$

In this case the solution of Eq. (2), $dN/dt = -\alpha' N/t^m$, gives $\ln N = -\frac{\alpha'}{1-m} t^{1-m} + c$, leading to a stretched exponential decrease of the drug particles remaining in the formulation, $N = N_0 \exp(-kt^b)$, with $b = 1 - m$ and $k = \frac{\alpha'}{1-m}$, while $N_0 = N(t = 0)$ is the initial number of drug particles in the formulation. Then the fractional release $(N_0 - N)/N_0 = M_t/M_\infty$ is given by Eq. (1), with a stretched exponential exponent

$$b = 1 - m \tag{4}$$

and a stretched exponential time parameter $\tau = k^{-1/b}$.

Here we test the validity of this argument by calculating the time dependence of the fraction of drug particles near the release boundary, which are able to exit the formulation per unit of time. In particular we examine whether Eq. (3) approximately holds during the release process or at least in a part of the release. Drug delivery devices of two different geometries, spheres and slabs, are considered. We perform Monte Carlo simulations to numerically investigate diffusion controlled drug release. Analytical results from the solution of diffusion equation are also discussed. We further check whether the obtained power-law exponent m of Eq. (3) and the corresponding stretched exponential exponent b derived through Eq. (4) are in accordance with results discussed in previous works [14,16], obtained through the direct fitting of release profiles with Eq. (1).

2 Results

2.1 Release from spherical devices

We start with the case of spherical drug delivery formulations. The formation of a concentration gradient during the release, with a smaller drug concentration near the

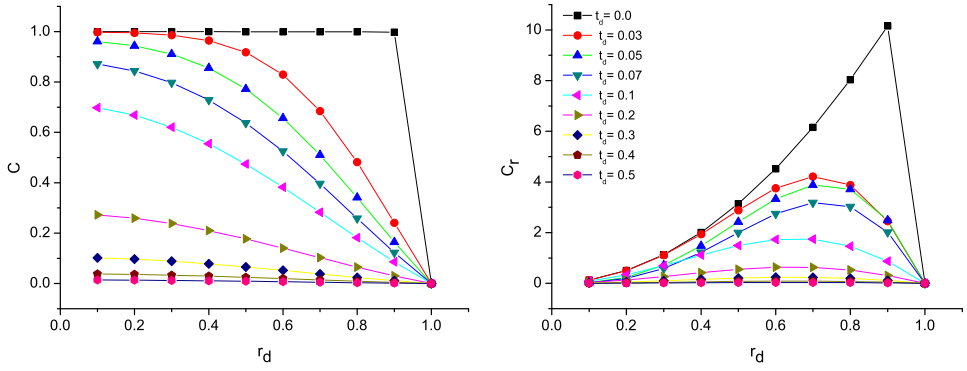

(a) (b)

Fig. 1. Evolution of the drug concentration pattern within a spherical formulation during the release process, as obtained from Eq. (5). (a) Concentration C and (b) radial concentration C_r, as a function of the dimensionless radial distance, $r_d = r/R$, from the center of sphere ($0 \leq r_d \leq 1$), at various dimensionless times $t_d = tD/R^2$ are shown by different symbols. The concentration values are normalized to the initial concentration C_0. Lines are guides to the eye.

boundary, is directly obtained from the analytical solution of diffusion equation (Fick's second law), $dC/dt = D \cdot \nabla^2 C$, where C is the number concentration of drug particles and D is the diffusion coefficient [29,30]. For a homogeneous initial distribution with a drug concentration C_0 in a sphere of radius R, the solution of diffusion equation assuming sink boundary conditions gives

$$C(r,t) = \frac{2C_0}{\pi(r/R)} \sum_{n=1}^{\infty} \frac{(-1)^{n+1}}{n} \sin\left(n\pi \frac{r}{R}\right) \cdot e^{-n^2\pi^2 \frac{D}{R^2} t}. \tag{5}$$

This expression provides the drug concentration inside the formulation, at a radial distance r from the center of sphere at any time t.

Considering dimensionless radial distance $r_d = r/R$ and time $t_d = (D/R^2)t$, we show in Fig. 1 the evolution of the drug concentration pattern as given by Eq. (5). In particular Fig. 1(a) depicts the normalized concentration C/C_0 as a function of r_d at different times t_d, while Fig. 1(b) shows the corresponding radial concentration $C_r = 4\pi r^2 C/C_0$. As it can be seen from Fig. 1(a), the initial homogeneous concentration at $t_d = 0$ quickly exhibits a distance dependence, through a depletion of drug particles near the boundary $r_d = 1$. A concentration gradient is developed, from the boundary towards the sphere center, during the release process. Concerning the radial concentration (Fig. 1(b)), the initial peak at the boundary rapidly moves inwards due to the escape of the particles close to the exit.

Using the analytical solution, Eq. (5), we can calculate the fraction of drug particles near the boundary. If N (M) is the number of particles (mass of drug molecules) inside the sphere at time t_d, and N_a (M_a) the corresponding number (mass) in a spherical shell of thickness a, extending from a distance a below the surface until the boundary, one obtains for the fraction $M_a/M = N_a/N$, in dimensionless units:

$$\frac{M_a}{M} = \frac{\int_{shell} C(r,t)dV}{\int_{sphere} C(r,t)dV} = \frac{\sum_{n=1}^{\infty} \frac{1}{n^3} e^{-n^2\pi^2 t_d} \left[n\pi - \sin(n\pi a) - n\pi(1-a)\cos(n\pi a)\right]}{\pi \sum_{n=1}^{\infty} \frac{1}{n^2} e^{-n^2\pi^2 t_d}} \tag{6}$$

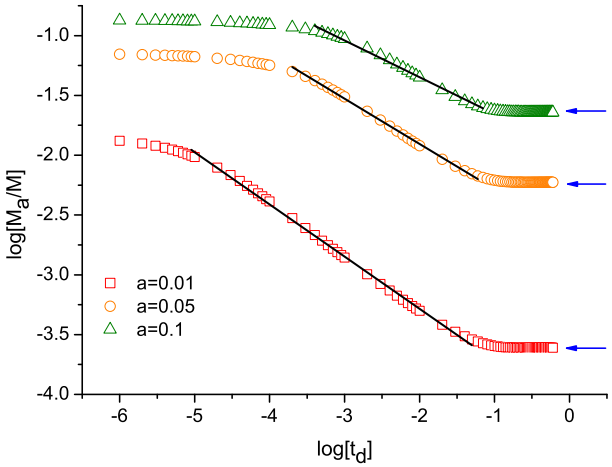

Fig. 2. Logarithm of the fraction of drug particles, M_a/M, in a shell of thickness a below the surface of the sphere as a function of the logarithm of the dimensionless time t_d, for different values of the dimensionless layer thickness a (points), as obtained from Eq. (6) by the analytical solution of Fick's second law. Solid lines represent decreasing linear parts, corresponding to a power-law dependence as given in Eq. (3). Arrows at the right of each plot show the analytically obtained limiting value at relatively long times (see text).

where $\int_{shell} C(r,t)dV = 4\pi \int_{1-a}^{1} r^2 C dr$ represents an integral over the shell of thickness a below the surface of the sphere and $\int_{sphere} C(r,t)dV = 4\pi \int_{0}^{1} r^2 C dr$ an integral over the whole sphere.

Figure 2 presents in logarithmic scale the time dependence of M_a/M, as given by Eq. (6), for different values of the thickness a of the boundary layer. We see that after a short initial period, a decreasing linear part appears (shown by solid lines in Fig. 2), denoting a t^{-m} dependence, in accordance to the assumption of Eq. (3). However this behavior does not last until the end of the release; a saturation at a constant value occurs in the last part of the process. This saturation value can be analytically obtained by Eq. (6), since at relatively long times the first term (for $n = 1$) dominates in the two sums in the nominator and denominator, leading to a limiting value of M_a/M equal to $1 - \frac{\sin(\pi a)}{\pi} - (1-a)\cos(\pi a)$. As shown by the arrows at the right of the corresponding plots, the latter formula indeed provides the saturation value observed at the last part of the release in Fig. 2.

The slope of the decaying linear part in Fig. 2 depends on the scale of the boundary layer (the value of a). Examining different values of a, it seems that there is not a limiting value of this slope in the dimensionless formalism considered. In the real problem (restoring back dimensional quantities), the specific length scale of the boundary layer determining the value of m (and thus the stretched exponential exponent $b = 1 - m$) is given by $\sqrt{6Dt}$ for $t = 1$ *time unit*. This is because a diffusive particle in a three-dimensional space travels a distance $\sqrt{6Dt}$ at time t and the boundary layer is defined as containing the drug particles that can escape per unit of time. Considering a spherical formulation with a radius $R = 1\,\mathrm{cm}$ and different values of D from 10^{-6}–$10^{-8}\,\mathrm{cm}^2/\mathrm{sec}$, we have checked that the dimensional form of Eq. (6), using a boundary layer of thickness $\sqrt{6D \times 1\,\mathrm{sec}}$, provides a decreasing linear part with a consistent value of the slope $m \approx 0.45$. This value compares well with the result 0.41 obtained by the numerical simulations for large values of R (see below).

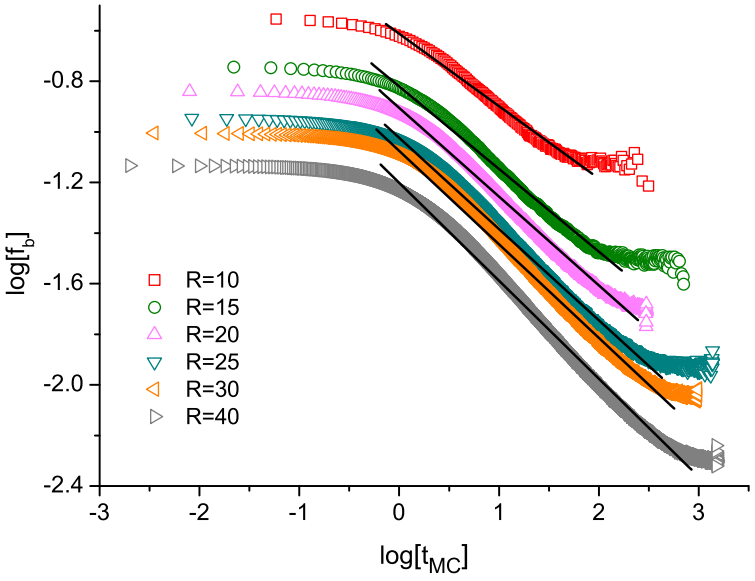

Fig. 3. Logarithm of the fraction f_b of drug particles that can reach an exit per unit of time (i.e. the fraction of particles located within one lattice spacing from the surface boundary) as a function of the logarithm of Monte Carlo time t_{MC}, for spheres of different radius R (points), calculated through MC simulations. Solid lines represent least squares fittings of the decreasing linear parts with straight lines, corresponding to a power-law dependence as given in Eq. (3).

A similar behavior as that presented in Fig. 2 is revealed by the numerical results obtained through Monte Carlo (MC) simulations. The Monte Carlo procedure used for simulating drug release from spheres makes use of a discrete three-dimensional lattice, representing the formulation, where the drug molecules diffuse and escape when they pass through the spherical boundary. Details of the method are given in Sect. 2.1 of [14]. In order to calculate the fraction $f_b(t)$ of drug molecules that can reach the surface boundary per unit of time, we take into account that the unit of time in the used MC scheme is the mean time required from the drug particles to move in a neighboring lattice site [14]. Therefore, to obtain $f_b(t)$ we compute during the MC simulation the number of occupied lattice sites within one lattice spacing from the surface boundary (corresponding to the release boundary layer), divided over the total number of occupied lattice sites inside the sphere.

Figure 3 presents the evolution of this quantity with the MC time, for spheres of different radii R. The results have been statistically averaged over 100 realizations in each case. As happens with the analytical results discussed above, also the numerical MC data show a $f_b(t) \sim t^{-m}$ dependence after an initial short time, followed by a saturation. Taking into account the release profile M_t/M_∞ as a function of MC time (data not shown here, see for example Fig. 2 in [14]), the obtained results in Fig. 3 show that the power-law dependence of Eq. (3) starts early during the process, at around 1–5% of the release, and lasts up to at least 80% of the release (reaching values above 90% in some cases). Therefore, a stretched exponential release kinetics is justified from very early during the process, up to the release of the large majority of drug molecules. Moreover, due to the correct asymptotic behavior at long times, the stretched exponential function seems to provide a rather good approximation for the overall release profile.

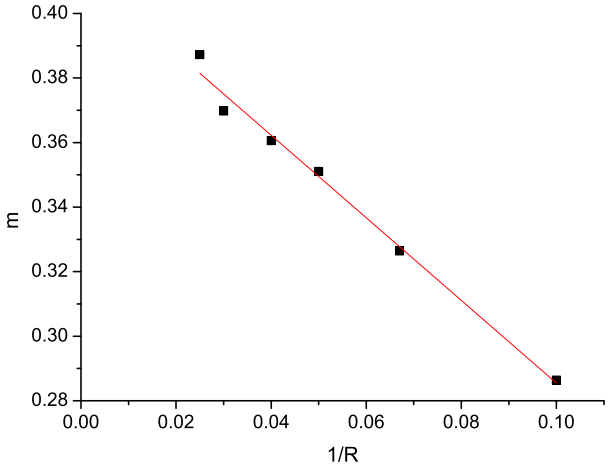

Fig. 4. The exponent m of the power-law $f_b(t) \sim t^{-m}$ as a function of the inverse radius R of the spherical delivery device (squares), as obtained from the numerical results presented in Fig. 3. Solid line shows a least square fit of the data.

We calculate next the values of the exponent m of the power-law, which can be derived by the results of the numerical simulations. These are obtained by the slopes of the least square fittings of the linear parts of $f_b(t)$ in the logarithmic plot of Fig. 3 (continuous lines). The results are depicted in Fig. 4, where the variation of the exponent m with the inverse sphere radius is presented. A linear dependence is shown by these data. A least square fitting gives that $m = 0.41 - \frac{1.3}{R}$. Then, Eq. (4) suggests that the stretched exponential exponent b is

$$b = 1 - m = 0.59 + \frac{1.3}{R}. \tag{7}$$

The last relation is in good agreement with the dependence $b = 0.61 + \frac{1.0}{R}$ that has been calculated in [14] through direct fitting of the release profiles, obtained by MC simulations, with Eq. (1).

2.2 Release from slabs

Now we consider diffusional drug release from slabs. The solution of the second law of Fick for a slab of thickness L, assuming sink boundary conditions, is

$$C(x,t) = \frac{4C_0}{\pi} \sum_{n=0}^{\infty} \frac{1}{2n+1} \sin\left[(2n+1)\pi \frac{x}{L}\right] \cdot e^{-(2n+1)^2 \pi^2 \frac{D}{L^2} t} \tag{8}$$

where the constant C_0 is the initial linear concentration of the number of drug particles (we assume homogeneous distribution at $t = 0$) and x is the direction of interest, perpendicular to the slab main surfaces at $x = 0$ and $x = L$.

Using again dimensionless units of distance, $x_d = x/L$, and time, $t_d = (D/L^2)t$, we present in Fig. 5 the drug concentration pattern inside the slab at different times t_d. A depletion of drug molecules near the two boundaries of the slab, at $x_d = 0$ and $x_d = 1$, and the development of concentration gradients towards the center at $x_d = 0.5$ is also observed in this case.

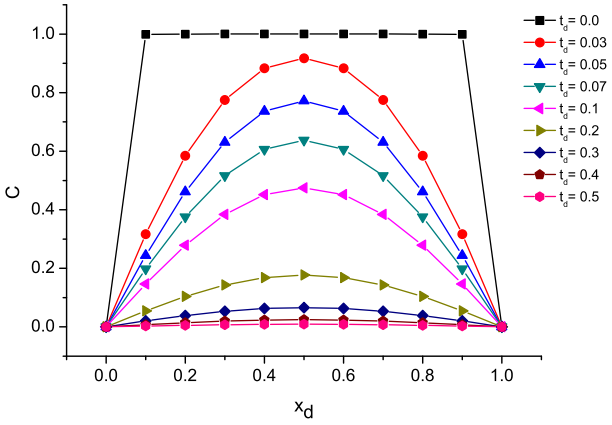

Fig. 5. Evolution of the drug concentration pattern inside a slab-shaped formulation during the release process, as obtained from Eq. (8). The concentration C as a function of the dimensionless distance, $x_d = x/L$, along the slab ($0 \leq x_d \leq 1$), at various dimensionless times $t_d = tD/L^2$ is shown by different symbols. The concentration values are normalized to the initial linear concentration C_0. Lines are guides to the eye.

From Eq. (8) the fraction of drug particles near the boundary, $M_a/M = N_a/N$, is readily obtained. Here N_a (M_a) is the number (mass) of drug molecules in two layers of thickness a at the two slab boundaries, which are close to an exit, and N (M) is the total number of particles (mass) inside the slab. In dimensionless units the result is

$$\frac{M_a}{M} = \frac{\int_{layers} C(x,t)dx}{\int_{slab} C(x,t)dx} = \frac{\sum_{n=0}^{\infty} \frac{1}{(2n+1)^2} e^{-(2n+1)^2\pi^2 t_d} \left[1 - \cos\left((2n+1)\pi a\right)\right]}{\sum_{n=0}^{\infty} \frac{1}{(2n+1)^2} e^{-(2n+1)^2\pi^2 t_d}}. \quad (9)$$

The integral $\int_{layers} C(x,t)dx = \int_0^a C dx + \int_{1-a}^1 C dx = 2\int_0^a C dx$ is over the two layers of thickness a attached to the surface boundaries, while the integral $\int_{slab} C(x,t)dx = \int_0^1 C dx$ is over the whole slab.

The temporal evolution of M_a/M given by Eq. (9) is shown in Fig. 6, for different values of the thickness a of the boundary layers. The plot exhibits the same features as those discussed previously in the case of spheres. The power-law t^{-m} dependence (denoted by straight continuous lines) appears after an initial short period. The saturation value at the last part of the release, obtained at relatively long times through the first terms (for $n = 0$) of the sums in the nominator and denominator of Eq. (9), is equal to $1 - \cos(\pi a)$ in this case. This result is shown by arrows at the right of the corresponding plots in Fig. 6. As noted previously, the dimensionless results do not show a limiting value of the slope that is independent on the boundary thickness a. Considering the dimensional quantities in a real problem, since the distance traveled at time t by a diffusive particle in the one-dimensional case is $\sqrt{2Dt}$, the specific length scale of the boundary layer (from where the drug molecules can escape per unit of time) is $\sqrt{2D \times 1\,\text{t.u.}}$, where t.u. denotes the *time unit*. Indeed using this value of boundary layer thickness, we have found that slabs with $L = 1$ cm and D ranging from 10^{-6}–10^{-8} cm^2/sec exhibit a similar slope $m \approx 0.44$ of the decreasing linear part in the logarithmic plot of M_a/M as a function of time in dimensional units. The corresponding MC result for large values of L is 0.39 as we see below.

We have also performed MC calculations to simulate release from slabs, using a three-dimensional lattice with periodic boundary conditions at the x- and y-axes and

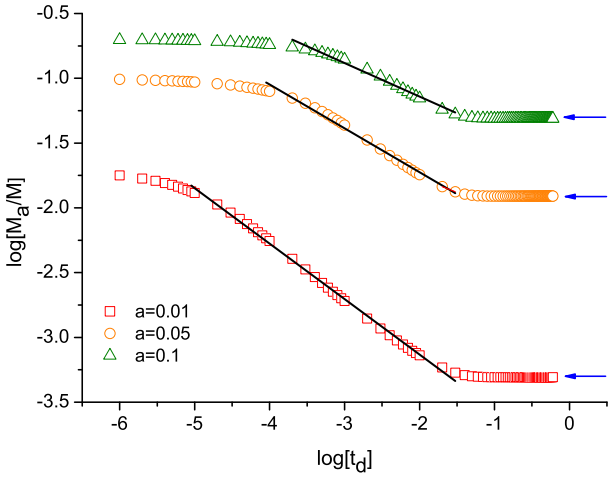

Fig. 6. Logarithm of the fraction of drug particles, M_a/M, in two layers of thickness a attached to the boundary surfaces of the slab as a function of the logarithm of the dimensionless time t_d, for different values of the dimensionless layer thickness a (points), as obtained from Eq. (9) by the analytical solution of diffusion equation. Solid lines represent decreasing linear parts, corresponding to a power-law dependence as given in Eq. (3). Arrows at the right of each plot show the analytically obtained limiting value $1 - \cos(\pi a)$ at relatively long times.

releasing direction along the z axis, as described in detail in Sect. 2.1 of [16] (the role of x in the analytical results discussed above is undertaken now by z). In order to find the fraction $f_b(t)$ of particles that can exit through the boundaries per unit of time, we calculate the number of occupied lattice sites at the top and bottom layers of the lattice at $z = L$ and $z = 0$, respectively (corresponding to the release boundary layers in this case), divided by the total number of occupied lattice sites of the slab. The time dependence of $f_b(t)$ for different values of the thickness L of the slab is presented in log-log plot in Fig. 7. Statistical averaging over 100 realizations has been used in each value of L. The $f_b \sim t^{-m}$ relation is confirmed again in this case for a substantial part of the release process . In particular, considering the release profile M_t/M_∞ (see Fig. 2 of [16]), we find that the power-law dependence appears around, or even below, 1% of the release and lasts up to more than 80% (above 90% for the larger values of L).

Through the slopes of the least square fittings of the linear parts of $f_b(t)$ in Fig. 7 (shown by solid lines in the corresponding plot), we compute the exponent m of the power-law. The dependence of this exponent on L is shown in Fig. 8, where a linear relation between m and the inverse slab thickness is obtained. A least square fit of the numerical results (solid line in Fig. 8) yields $m = 0.39 - \frac{1.7}{L}$. Then, the stretched exponential exponent b of the release curve, obtained by Eq. (4), is

$$b = 1 - m = 0.61 + \frac{1.7}{L}. \tag{10}$$

In [16], the fitting of the MC simulated release profiles with Eq. (1) has led to the relation $b = 0.71 + \frac{1.1}{L}$.

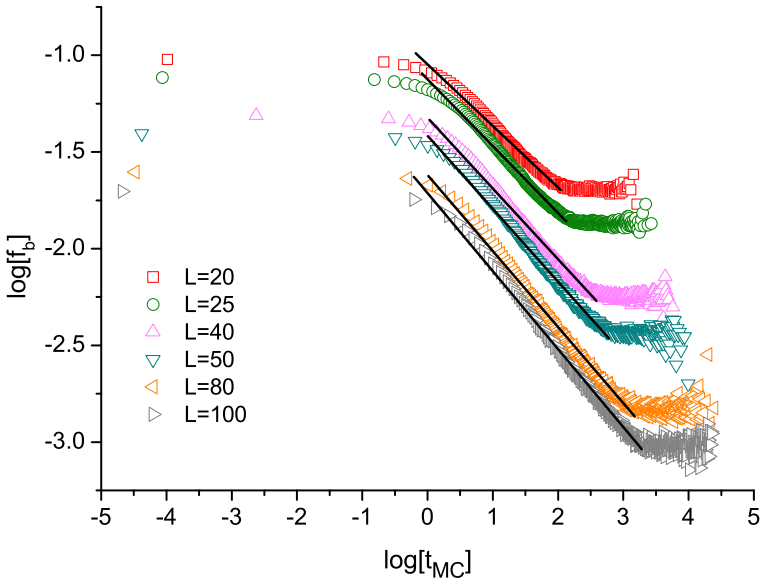

Fig. 7. Logarithm of the fraction f_b of drug particles that can escape per unit of time (i.e. the fraction of particles located at the top and bottom layers of the lattice representing the slab) as a function of the logarithm of Monte Carlo time t_{MC}, for slabs of different thickness L (points), calculated through MC simulations. Continuous lines represent least square fittings of the decreasing linear parts with straight lines, corresponding to a power-law dependence as given in Eq. (3).

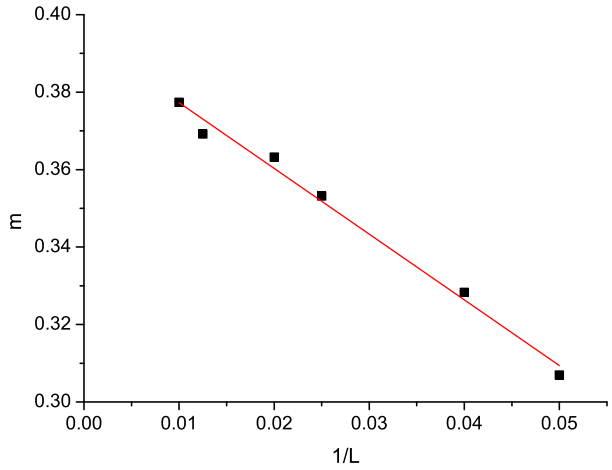

Fig. 8. The exponent m of the power-law $f_b(t) \sim t^{-m}$ as a function of the inverse thickness L of the slab (squares), as obtained from the numerical results presented in Fig. 7. Solid line shows a least square fit of the data.

3 Conclusions

We have examined diffusional drug release from spheres and slabs in order to calculate the fraction of drug molecules close to the boundaries, which can escape from the delivery device per unit of time. Analytical results from the solution of diffusion equation and numerical calculations using Monte Carlo simulations are discussed in this context.

The fraction of drug molecules near the boundaries exhibits an approximate power-law t^{-m} dependence in a substantial part of the release process. This behavior appears very early (around the 1–5% of the release) and lasts up to at least 80% of the release. Such a dependence underlies the theoretical derivation of a stretched exponential release kinetics. Taking into account that the stretched exponential function exhibits the correct asymptotic description of a release problem at long times, this justifies the use of the Weibull function as an approximate description of the overall release profile, in accordance with the results presented in a number of previous studies.

This work has been partially supported by the Thales project MACOMSYS, co-financed by the European Union (ESF) and the Greek Ministry of Education (through the $E\Sigma\Pi A$ program), and by European Union's Seventh Framework Programme (FP7-REGPOT-2012-2013-1) under grant agreement no 316165.

References

1. V. Papadopoulou, K. Kosmidis, M. Vlachou, P. Macheras, Int. J. Pharm. **309**, 44 (2006)
2. U. Gbureck, E. Vorndran, J.E. Barralet, Acta Biomater. **4**, 1480 (2008)
3. G.F. Picheth, M.R. Sierakowski, M.A. Woehl, L. Ono, A.R. Cofre, L.P. Vanin, R. Pontarolo, R.A. De Freitas, J. Pharm. Sci. **103**, 3958 (2014)
4. M. Spanakis, N. Bouropoulos, D. Theodoropoulos, et al., Nanomedicine: NBM **10**, 197 (2014)
5. M. Bartzegar-Jalali, K. Adibkia, H. Valizadeh, et al., J. Pharm. Pharmaceut. Sci. **11**, 167 (2008)
6. K. Kosmidis, P. Argyrakis, P. Macheras, Pharm. Res. **20**, 988 (2003)
7. K. Kosmidis, P. Argyrakis, P. Macheras, J. Chem. Phys. **119**, 6373 (2003)
8. P. Macheras, A. Iliadis, *Modeling in Biopharmaceutics, Pharmacokinetics, and Pharmacodynamics: Homogeneous and Heterogeneous Approaches* (Springer, New York, 2006)
9. R. Villalobos, A.M. Vidales, S. Cordero, D. Quintanar, A. Dominguez, J. Sol-Gel Sci. Technol. **37**, 195 (2006)
10. R. Villalobos, S. Cordero, A.M. Vidales, A. Dominguez, Physica A **367**, 305 (2006)
11. K. Kosmidis, P. Macheras, Int. J. Pharm. **343**, 166 (2007)
12. K. Kosmidis, P. Macheras, Int. J. Pharm. **354**, 111 (2008)
13. L. Martinez, R. Villalobos, M. Sanchez, J. Cruz, A. Ganem, L.M. Melgoza, Int. J. Pharm. **369**, 38 (2009)
14. A. Hadjitheodorou, G. Kalosakas, Mater. Sci. Eng. C **33**, 763 (2013)
15. A. Hadjitheodorou, G. Kalosakas, Mater. Sci. Eng. C **42**, 681 (2014)
16. G. Kalosakas, D. Martini, Int. J. Pharm. **496**, 291 (2015)
17. S. Casault, G.W. Slater, Int. J. Pharm. **365**, 214 (2009)
18. T. Higuchi, J. Pharm. Sci. **50**, 874 (1961)
19. J. Siepmann, N.A. Peppas, Int. J. Pharm. **418**, 6 (2011)
20. N.A. Peppas, Pharm. Acta Helv. **60**, 110 (1985)
21. P.L. Ritger, N.A. Peppas, J. Control. Release **5**, 23 (1987)
22. P.L. Ritger, N.A. Peppas, J. Control. Release **5**, 37 (1987)
23. N.A. Peppas, B. Narasimhan, J. Control. Release **190**, 75 (2014)
24. P. Costa, J.M.S. Lobo, Eur. J. Pharm. Sci. **13**, 123 (2001)
25. A. Dokoumetzidis, P. Macheras, Int. J. Pharm. **321**, 1 (2006)
26. S. Casault, G.W. Slater, Physica A **387**, 5387 (2008)
27. S. Dash, P.N. Murthy, L. Nath, P. Chowdhury, Acta Pol. Pharm. **67**, 217 (2010)
28. N. Pippa, A. Dokoumetzidis, S. Pispas, C. Demetzos, Int. J. Pharm. **465**, 63 (2014)
29. H.S. Carlslaw, J.C. Jaeger, *Conduction of Heat in Solids* (Oxford University Press, 1959)
30. J. Crank, *The Mathematics of Diffusion*, 2nd ed. (Oxford University Press, 1980)